

INVESTIGATION OF THE LIGHT YIELD OF LUMINESCENT SCREENS FOR HIGH ENERGY AND HIGH BRILLIANT ELECTRON BEAMS

G. Kube, DESY, Hamburg, Germany
 W. Lauth, Institut für Kernphysik, Mainz, Germany

Abstract

Transverse beam profile diagnostics at electron accelerators is usually performed with optical transition radiation (OTR) monitors. For intense beams however, thermal load in the screen material may result in resolution degradation and even screen damage. To overcome this problem the beam can be swept over the screen, but the strong OTR light emission directivity will reduce the optical system's collection efficiency. In order to overcome these difficulties, luminescent screens can be used because of their robustness and isotropic light emission. Since only little information is available about scintillator properties for applications with high energy electrons, a test experiment has been performed in order to study the light yield of different screen materials under electron bombardment.

INTRODUCTION

For the European XFEL with a maximum beam energy of 20 GeV and an average beam power of up to 300 kW it is planned to install a beam profile monitor in the dump section in order to control beam position and size and to avoid damage of the dump window. OTR is widely used for transverse beam profile measurements with high energy electrons. Advantages of OTR are the radiation generation directly at the screen boundary in an instantaneous emission process, and the rather high light output emitted in a small lobe with an opening angle defined by the beam energy. For intense beams however, the thermal load from the particle interaction with the screen material results in a degradation of the image resolution and possible screen damage. To overcome this problem the beam can be swept over the screen, but in this case the strong OTR light emission directivity has the drawback of reducing the collection efficiency of the optical system. Therefore it is planned to use luminescent screens because of their robustness and isotropic light emission. While the use of luminescent screens at hadron machines is widespread (see e.g. Refs. [1, 2] and the references therein), there is little information about scintillator properties for applications with high energy electrons. At the SLC linac for example, screens based on phosphor ($\text{Gd}_2\text{O}_2\text{S:Tb}$ or P43) deposited on a thin aluminum foil were in use, showing no sign of damage after bombardment with up to 4×10^{18} e/cm² [3]. To study the light yield of other scintillator materials, a test experiment has been performed which is described in the following.

05 Beam Profile and Optical Monitors

EXPERIMENTAL SETUP

Figure 1 shows the sketch of the experimental setup. The experiment was performed at the 855 MeV beam of the Mainz Microtron MAMI (University of Mainz, Germany) [4] in the beamline of the X1 collaboration, close to the beam dump which is located behind the vertical deflecting bending magnet BM2. The screens were mounted directly

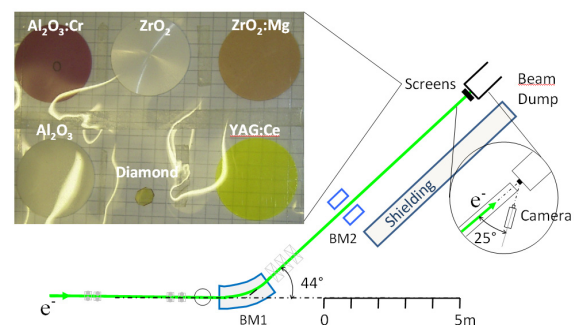


Figure 1: Screen test set-up in the X1 beamline at MAMI. The inset shows a photo of the screen materials under investigation.

in front of the dump in air. During beam exposure which lasted approximately one minute with a cw beam current of a few nA, the emitted luminescence light was observed via a standard Vidicon camera. The camera was located at a distance of about 1 m from the screens such that the loss of scintillation light intensity due to total reflection in the screen material was neglectable.

Table 1: Overview of the Screen Materials and Thicknesses Together with the Applied Beam Current

material	d / mm	current / nA
YAG:Ce	1	0.5
Diamond	0.2	1.9
Al ₂ O ₃	1	1.9
Al ₂ O ₃ :Cr (Chromox)	1	0.5
ZrO ₂ (Z700-20A)	1	32.4
ZrO ₂ :Mg (Z507)	1	32.4

Six different screens have been tested which are listed in Table 1 together with their thickness and the applied cw beam current. An industrial diamond crystal (Sumitomo Electric Industries [6]) together with four ceramic screens (BCE Special Ceramics [7]) were investigated with respect to their luminescence yield. The YAG:Ce crystal (Saint

Gobain Crystals [5]) served as reference.

DATA TAKING AND ANALYSIS

For each scintillator material, 10 images were taken with and 5 without beam. Each resulting mean background image was subtracted from the corresponding mean signal image in order to determine the background corrected profile image. The resulting image was normalized to the cw current according to Table 1 and then fitted in a pre-defined range of interest (ROI) with a normal distribution. Figure 2 shows the fit result for the Al_2O_3 screen as an example. Afterwards the light yield was determined by summing up the background corrected normalized intensity over a range of $\pm 6\sigma$ with respect to the profile maximum.

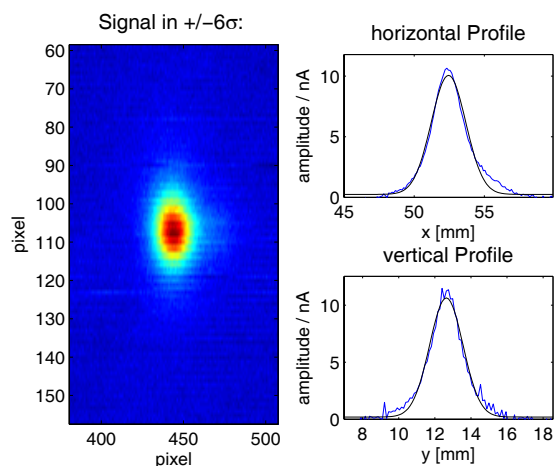


Figure 2: Left: background corrected beam image in range of interest for intensity integration. Right: normalized projected beam profiles and fit with normal distribution.

The results are summarized in Table 2. The horizontal and vertical (1σ) widths from the fit in the central parts of the projected profiles are listed together with the relative intensities, integrated over the corresponding ROIs. The intensities are expressed in units of the YAG:Ce intensity.

Table 2: Horizontal and Vertical (1σ) Widths Together with the Integrated Normalized Intensities for each Screen Material

material	σ_x [mm]	σ_y [mm]	I_{norm} [a.u.]
YAG:Ce	0.91	0.77	1
Chromox	0.93	0.73	72.6×10^{-3}
Al_2O_3	1.04	0.80	41.8×10^{-3}
Diamond	-	-	24.9×10^{-3}
$\text{ZrO}_2\text{:Mg}$	0.67	0.46	1.6×10^{-3}
ZrO_2	0.86	0.62	0.6×10^{-3}

The diamond crystal showed intense luminescence effects, and a light spot was clearly visible. However, due

to its small size (c.f. Fig 1), part of the light was reflected at the crystal boundaries and some could even escape out of its volume. Therefore it was not possible to determine the projected profiles, and in the subsequent analysis this measurement will not be considered.

In case of the YAG crystal the $\pm 6\sigma$ range for intensity integration was not sufficient. As can be seen from Fig. 3 the profile no longer resembles a normal distribution and the intensity contribution in the tails is larger than in the measured profiles with other screens, see e.g. Fig. 2. The strong asymmetry is due to the fact that the beam was hitting the crystal close to its border and the range of light emission is restricted to the crystal volume. In order to account for this intensity loss for the light yield determination, the intensity integral from the profile maximum to -17σ was determined and the result was multiplied by a factor of 2.

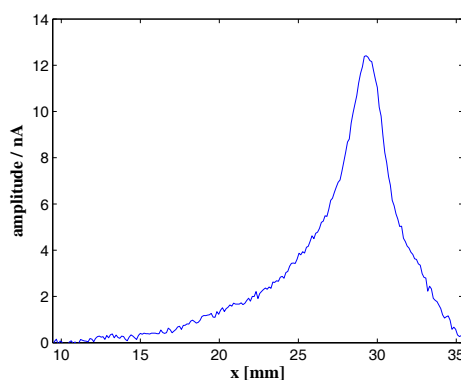


Figure 3: Horizontal profile as measured with the YAG:Ce screen.

The effect of image blurring in profile diagnostics with YAG screens is reported in Refs. [8, 9, 10] and explained by saturation of the scintillating sites inside the crystal and space charge ionization enhancement. For this experiment however, an effect due to saturation doesn't seem applicable because of the low beam charge density and the fact that a fit of the central part of the profile with a normal distribution results in profile widths comparable to those from the other screens, see Table 2. It is more likely that the increased intensity in the tails is due to light reflection from the backside of the scintillator crystal. However, the explanation of this effect needs further investigation.

Comparing the transverse beam sizes in Table 2 it is striking that the results of the measurements with ZrO_2 ceramics are both smaller than the others. Furthermore, during the course of the experiment it was possible to observe immediately a discolouration of the screen at the positions where the beam hits the ceramics, c.f. Fig. 4. By heating the samples at 150° in air for a few hours both screens recovered. After the irradiation which lasted only about one minute per target, both screens showed additionally a strong activation in the order of $30 \mu\text{Sv/h}$. As consequence the use of ZrO_2 screens seems not to be suitable for electron beam diagnostics.

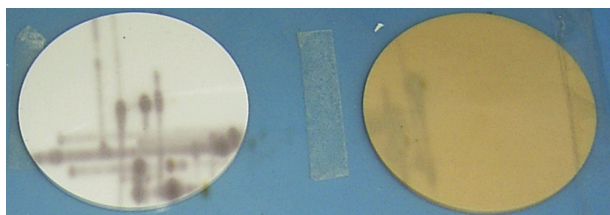


Figure 4: ZrO_2 screen (left) and $\text{ZrO}_2\text{:Mg}$ screen (right) after electron bombardment. The positions where the beam hits the ceramics are clearly visible as dark spots or lines.

Efficiency Estimation

In this subsection a rough estimate for the scintillator efficiency will be given. While the intention of the test experiment was not to measure absolute values, the estimation is based on published values for the YAG:Ce efficiency as reference together with simplified experimental assumptions:

For the light yield of YAG:Ce crystals values between 8 [5] and 20.3 photons/keV [11] can be found in the literature. For the following analysis an efficiency of 8 photons/keV is assumed because it is the value as quoted from the crystal supplier.

Furthermore, to simplify it is assumed that the difference in the scintillator light outputs is caused by the different energy depositions of the beam electrons in the scintillator materials. None of the screens under investigation belongs to the category of cross-luminescent scintillators, therefore the processes of energy conversion (i.e. the formation of 'hot' electrons and holes in the scintillator host material), their thermalization, and the energy transfer to the luminescent centers (either extrinsic, i.e. doping ions, or intrinsic) were considered to be the same for all materials. The energy deposition is calculated with the Geant4 code [12] under the assumption that the energy loss is caused by the host material, and not by the activators because of their small concentration.

Table 3 summarizes the estimated light yield for the scintillators under investigation. Additionally it is assumed that

Table 3: Estimated Scintillator Efficiencies Together with Calculated Deposited Energy According to Ref. [12]

material	ΔE [keV]	light yield [photons/keV]
YAG:Ce	680	8 (Ref. [5])
Chromox	619	0.639
Al_2O_3	619	0.367
$\text{ZrO}_2\text{:Mg}$	829	0.011
ZrO_2	829	0.004

the camera sensitivity is constant, i.e. the emission spectrum of the individual scintillators is not taken into account.

Finally the self absorption inside the scintillator material is not taken into account, i.e. the luminescent light emission originates from the entire scintillator thickness. According to Ref. [13] it is a general scintillator property

to be transparent in the sense that energy levels involved in the radiative transition are contained in the forbidden energy band to avoid reabsorption of the emitted light or photo-ionization of luminescent centers.

CONCLUSION

As can be concluded from Table 3 the YAG:Ce screen provides the highest output, more than one order of magnitude compared to a Chromox ceramic. However, the measured beam shape from the YAG screen was distorted, the reason for this profile degradation needs further investigation. With simplified assumptions the light yield difference between Chromox and the standard Al_2O_3 ceramic for electron bombardment amounts to only a factor of 2. For heavy ion bombardment, on the other hand, it was found out that a Chromox screen gives about one order of magnitude more intensity than an Al_2O_3 ceramic [14]. Finally the use of ZrO_2 ceramics seems not to be suitable for electron beam diagnostics because of the low light output, the material degradation under bombardment, and the rather high screen activation.

ACKNOWLEDGMENT

The authors would thank T. Hoffmann and E. Gütlich (GSI Darmstadt) for providing the YAG screen and the ceramic scintillators, B. Struth (DESY-HASYLAB) for providing the diamond crystal, and S. Weisse (DESY Zeuthen) for support with the camera server.

REFERENCES

- [1] R. Jung, G. Ferioli, and S. Hutchins, Proc. DIPAC'03, Mainz, Germany, May 2003, IT03, p.10 (2003).
- [2] C. Bal *et al.*, Proc. DIPAC'05, Lyon, France, June 2005, POM013, p.57 (2005).
- [3] M. Ross *et al.*, SLAC_PUB_3640 (1985).
- [4] J. Ahrens *et al.*, Nuclear Physics News **4** (1994) 5.
- [5] <http://www.detectors.saint-gobain.com>.
- [6] <http://www.sei.co.jp/index.en.html>.
- [7] <http://www.bce-special-ceramics.de/index.html>.
- [8] A.H. Lumpkin *et al.*, Nucl. Instr. and Meth. **A 429** (1999) 336.
- [9] A. Murokh *et al.*, Proc. 2nd ICFA Advanced Accelerator Workshop on the Physics of High Brightness Beams, p.564 (2000).
- [10] A. Murokh *et al.*, Proc. PAC'01, Chicago, Illinois, June 2001, p.1333 (2001).
- [11] M. Moszyński *et al.*, Nucl. Instr. and Meth. **A 345** (1994) 461.
- [12] S. Agostinell *et al.*, Nucl. Instr. and Meth. **A 506** (2003) 250. J. Allison *et al.*, IEEE Trans. Nucl. Sci. **53** No. 1 (2006).
- [13] P. Lecoq *et al.*, *Inorganic Scintillators for Detector Systems*, (Springer Verlag, Berlin-Heidelberg, 2006).
- [14] E. Gütlich, Diploma Thesis (in German), Fachhochschule Wiesbaden (Germany) 2008.